JOURNAL OF Materials CHEMISTRY

Lead-free ferroelectric relaxor ceramics in the $BaTiO_3$–$BaZrO_3$–$CaTiO_3$ system

Jean Ravez,* Cédric Broustera and Annie Simon

ICMCB-CNRS, 87 avenue Dr A. Schweitzer–33608 Pessac, France

Received 12th March 1999, Accepted 28th April 1999

Relative permittivity studies of ceramics with a variety of compositions in the $BaTiO_3$–$BaZrO_3$–$CaTiO_3$ system showed some of them to be ferroelectric relaxors at temperatures close to 295 K. Such a favourable effect is due to the Ca^{2+} for Ba^{2+} cationic substitution. In addition a spontaneous classical ferroelectric–relaxor ferroelectric transition was evidenced. Some of these new compositions are of interest for applications (dielectrics for capacitors, actuators) since they are environmentally friendly.

Introduction

In perovskites, relaxor behaviour mainly occurs in lead-based compositions (PMN, PSN, PIN, PLZT, *etc.*), with more than one type of ion occupying the equivalent six-coordinated crystallographic sites.[1] Lead-free compositions could be of great interest for environmentally friendly applications (dielectrics for capacitors, actuators, *etc.*). Studies have therefore been performed in detail on ceramics with a $BaTiO_3$-derived $Ba(Ti_{1-x}Zr_x)O_3$ composition. These materials are either classical or relaxor ferroelectrics depending on the value of x. Nevertheless, for all lead-free materials, the relaxor properties unfortunately occur at relatively low temperature ($T_m < 250$ K; T_m is the temperature of the peak of the relative real permittivity ε'_r *vs.* temperature; relative permittivity, $\varepsilon_r = \varepsilon/\varepsilon_0$).[2–12]

Research is now in progress to obtain such lead-free ceramics which could be relaxors at temperatures close to 300 K. The present study concerns compositions relatively close to that of $BaTiO_3$ in the ternary diagram $BaTiO_3$–$BaZrO_3$–$CaTiO_3$ [BT–BZ–CT]. The perovskite phase in the binary systems $(1-x)$ BT–x CT and $(1-x)$ BT–x BZ is limited to $x = 0.25$ and 0.42 respectively.[2,13]

Experimental

The various compositions of the BT–BZ–CT ternary diagram were obtained from $CaCO_3$, $BaCO_3$, TiO_2 and ZrO_2 after calcination at 1200 °C for 15 h under oxygen. Disk-shaped ceramics were sintered at 1400 °C for 4 h under an oxygen atmosphere. Some ceramics were prepared after addition of 1% TiO_2 excess (in mole) used as a sintering aid.[2] This amount of additive was selected after several experiments using various quantities (0.2 to 3% in mole) of certain oxides or fluorides.

Room temperature powder X-ray diffraction was performed on a Philips diffractometer using Cu-Kα radiation ($\lambda =$ 1.5418 Å), to measure Bragg angles from 5 to 100°. Diameter shrinkages $\Delta\Phi/\Phi$ were systematically determined as $(\Phi_{init} - \Phi_{final})/\Phi_{init}$. Microstructure studies were performed by scanning electron microscopy (SEM) (JEOL JSM-840A).

Measurements of relative permittivity were performed on ceramic disks after deposition of gold electrodes on the circular faces by cathodic sputtering. The real and imaginary relative permittivities ε'_r and ε''_r were determined under helium as a function of both temperature (77–500 K) and frequency ($20–2 \times 10^5$ Hz) using a Wayne-Kerr 6425 component analyzer.

Results

Physical properties

Powder X-ray diffraction made it possible to determine the room temperature symmetry and limits of the perovskite solid solution domain close to BT (Fig. 1). The symmetry is tetragonal only for compositions close to BT. In most of the other compositions the phases appear as cubic at 300 K. The various zones noted I, II and III are clarified in the dielectric section. The diameter shrinkages $\Delta\Phi/\Phi$ of the ceramics are in the range 14–16%. The densities of the sintered samples were 88–91% of the theoretical values. Concerning the ceramics prepared with TiO_2 as sintering aid, the diameter shrinkages were close to 19%. The densities of the samples reached 96% of the theoretical values, in good agreement with previous work.[2] In addition, the additive causes an increase in the grain size of the ceramics.

Dielectric study and ferroelectric properties

Depending on the composition (Fig. 1), three different types of behaviour were found.

For compositions relatively close to both BT and the $(Ba_{1-x}Ca_x)TiO_3$ [BT–CT] solid solution (zone I), there were dielectric anomalies characteristic of the phase transitions, as for BT (rhombohedral, $T_1 \rightarrow$orthorhombic, $T_2 \rightarrow$tetragonal, $T_C \rightarrow$cubic). In fact, the temperature dependence of the real part of the relative permittivity ε'_r revealed three maxima corresponding to these three phase transitions for compositions very close to that of BT. When the rate of Ca^{2+}–Ba^{2+} substitution increased, T_1 decreased strongly as for the BT–CT solid solution and only T_2 and T_C were detectable, owing to our experimental low temperature limitation ($T > 77$ K).[13] The

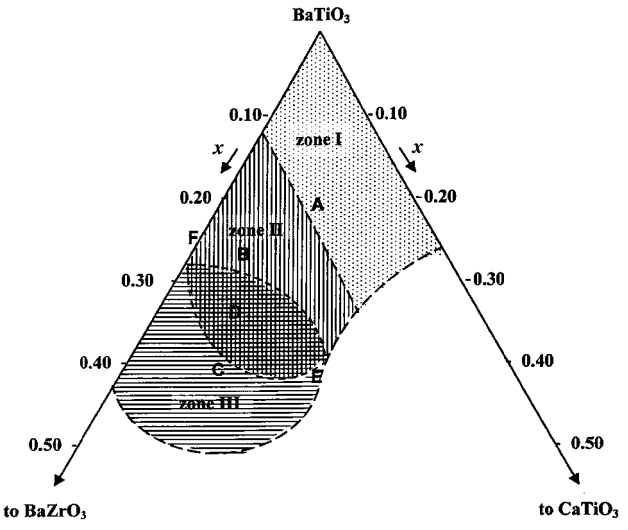

Fig. 1 Schematic representation of the BT–BZ–CT ternary diagram.

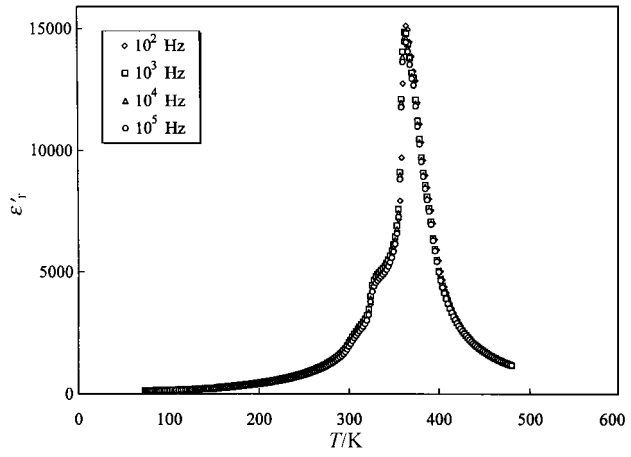

Fig. 2 Temperature dependence of relative permittivity ε'_r for a ceramic with composition corresponding to point A on Fig. 1.

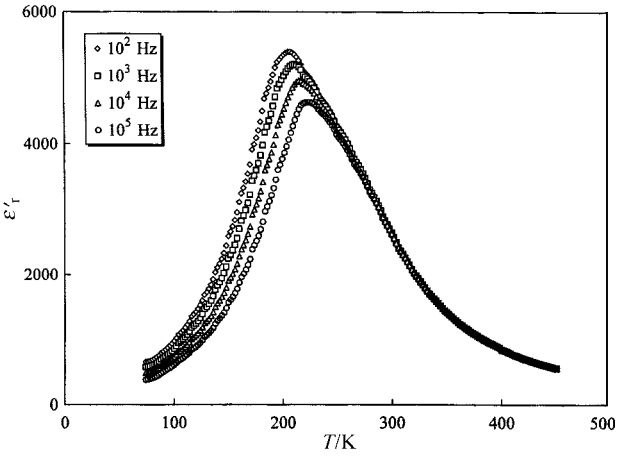

Fig. 4 Temperature dependence of relative permittivity ε'_r for a ceramic with composition corresponding to point C on Fig. 1.

tetragonal symmetry observed by room temperature X-ray diffraction corresponded to compositions whose Curie temperature T_C was higher than 300 K. For example Fig. 2 shows the temperature dependence of ε'_r for a ceramic with a composition corresponding to point A on Fig. 1. There is no significant frequency dispersion for $T < T_C$. The highest temperature peak at the Curie temperature T_C is relatively sharp and the value of T_C is not dependent on frequency. In addition, the thermal variation of $1/\varepsilon'_r$ is of the Curie–Weiss type: $\varepsilon'_r = C/(T - T_0)$ where C is the Curie constant and T_0 the Curie–Weiss temperature. The order of the ferroelectric–paraelectric transition can be determined from the temperature dependence of $1/\varepsilon'_r$. When T_0 is less than T_C the phase transition is of the first order; when $T_0 = T_C$ it is of second order. In fact, the phase transition order, which is of the first order for BT, moves progressively to the second order as the composition shifts from BT in zone I. All these physical properties point to a classical ferroelectricity as found in pure $BaTiO_3$.[9]

For compositions relatively close to the $Ba(Ti_{1-x}Zr_x)O_3$ [BT–BZ] solid solution with $0.10 \leqslant x \leqslant 0.27$ (zone II) only one peak occurred at the Curie temperature T_C. Fig. 3 shows the temperature dependence of ε'_r for a ceramic with a composition corresponding to point B on Fig. 1. There is no frequency dispersion. The value of ε'_r is very high at T_C. However, the peak of ε'_r *vs.* temperature is relatively broader than that corresponding to compositions close to $BaTiO_3$, and there is a small deviation from the Curie–Weiss law in the paraelectric phase. Such a behaviour indicates the transition is relatively diffuse but that the ferroelectric phase is not a relaxor.

For compositions relatively close to the $Ba(Ti_{1-x}Zr_x)O_3$ solid solution with $0.275 \leqslant x \leqslant 0.42$ (zone III) only one very broad peak occurred at T_m, with frequency dispersion for $T < T_m$ and a shift of T_m with frequency. The value of T_m (ferroelectric relaxor) is dependent on the frequency unlike that of T_C (classical ferroelectric). Figs. 4 and 5 show the temperature dependences of ε'_r and ε''_r for a ceramic with a composition corresponding to point C on Fig. 1. The frequency dispersion of ε'_r corresponds to a relatively high value of ε''_r for the relaxor phase ($T = 180$ K $< T_m$); on the contrary, ε'_r does not vary with frequency and ε''_r is very weak when $T = 300$ K $> T_m$ (Fig. 6). In addition, there is a deviation from the Curie–Weiss law generally observed in classical ferroelectrics and the value of T_0 here is higher than T_m. This is unlike classical ferroelectric behaviour where T_0 is either less than T_C or equal to T_C (Fig. 7). In this case, the ferroelectric–paraelectric transition is diffuse and the ferroelectric behaviour is thus of relaxor type.

For compositions corresponding to a wide boundary between zones II and III in the BT–BZ–CT system (Fig. 1) a new type of dielectric behavior was observed. Fig. 8 shows the temperature dependence of ε'_r for a ceramic with a composition corresponding to point D on Fig. 1. There is a relatively broad peak of ε'_r at T_m. On cooling a frequency dispersion appears at $T = T_m$. In addition, there is an increase in T_m when frequency increases. This behaviour is of relaxor type. However, the frequency dispersion decreases strongly in comparison to that observed at a temperature close to T_m, when the temperature is still decreasing. Moreover, it deviates

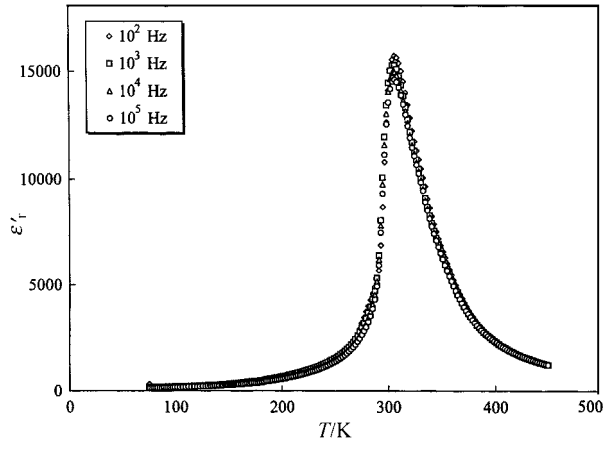

Fig. 3 Temperature dependence of relative permittivity ε'_r for a ceramic with composition corresponding to point B on Fig. 1.

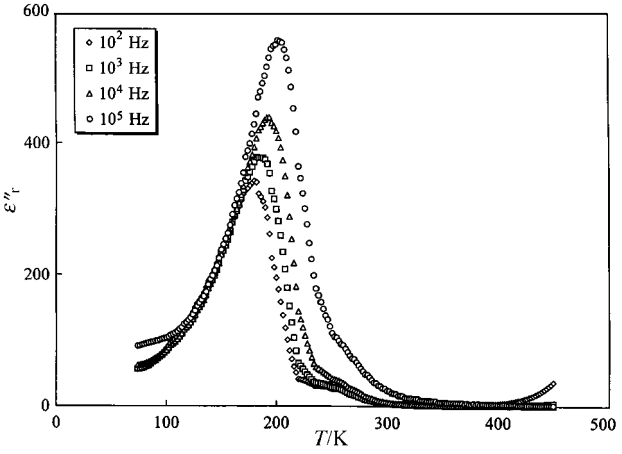

Fig. 5 Temperature dependence of the imaginary part of relative permittivity ε''_r for a ceramic with composition corresponding to point C on Fig. 1.

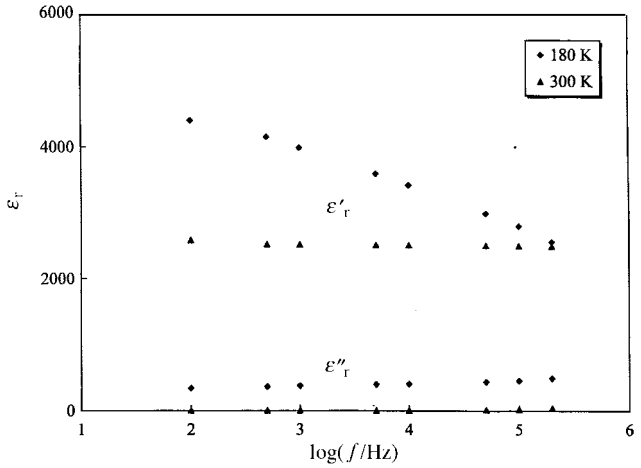

Fig. 6 Frequency dependences of relative permittivities ε'_r and ε''_r for a ceramic with composition corresponding to point C on Fig. 1.

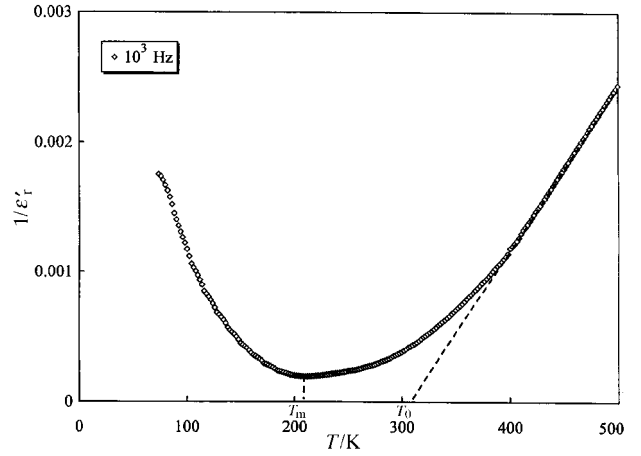

Fig. 7 Temperature dependence of the inverse of relative permittivity $1/\varepsilon'_r$ at 10^3 Hz for a ceramic with composition corresponding to point C on Fig. 1.

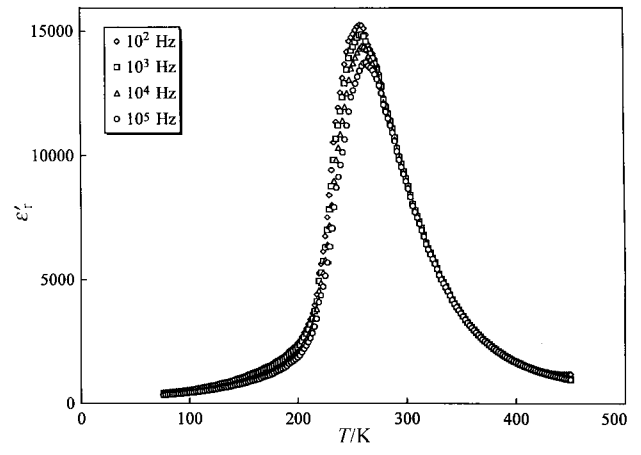

Fig. 8 Temperature dependence of relative permittivity ε'_r for a ceramic with composition corresponding to point D on Fig. 1.

strongly from T_m implying that the corresponding low temperature phase is of classical ferroelectric type. This gives the following transition sequence: classical ferroelectric, $T_3 \rightarrow$relaxor ferroelectric, $T_m \rightarrow$paraelectric. The term T_3 is used to differentiate it from T_1, T_2 and T_C, the transition temperatures of classical ferroelectrics derived from $BaTiO_3$ (see above) and from T_m the temperature of the maximum of ε'_r for a ferroelectric relaxor–paraelectric transition.

Some compositions of zone III meet the Z5U capacitor

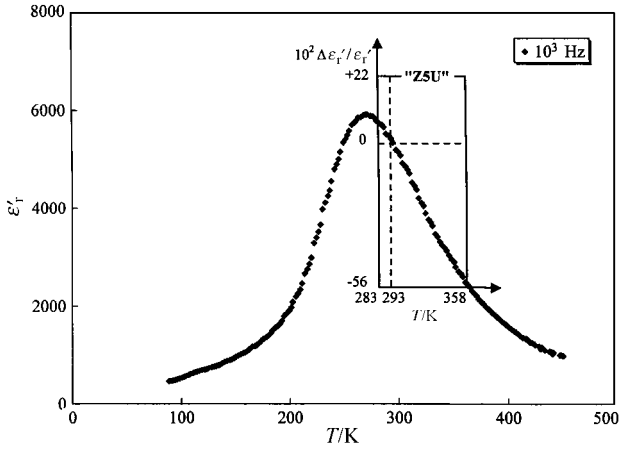

Fig. 9 Temperature dependence of relative permittivity ε'_r for a ceramic with composition corresponding to point E on Fig. 1 [Capacitor Z5U standard] [$\Delta\varepsilon'_r/\varepsilon'_r = \varepsilon'_r(T) - \varepsilon'_r$ (293 K)/ε'_r (293 K)].

'Electronic Industries Association' norm due to the broad peak of ε'_r as a function of temperature, to the relatively high value of ε'_r and to the low value of tan δ at 300 K.[14] Fig. 9 shows the temperature dependence of ε'_r (at 10^3 Hz) for a ceramic corresponding to point E on Fig. 1.

Moreover, very high values of ε'_r were obtained on zone II ceramics prepared after addition of 1% TiO_2 excess (in mole) used as sintering aid.[2] Fig. 10 shows the thermal variation of ε'_r, at 10^3 Hz, for a composition corresponding to point F on Fig. 1; the curve obtained with the ceramic sintered without any additive is given for comparison. The highest value of ε'_r at T_C reaches 42400 at 10^3 Hz. The room temperature values of ε'_r and tan δ are 28000 and 0.01 respectively. Such a result is due to the very good densification of the ceramic, in good agreement with previous work.[2]

Discussion

Ceramics with compositions forming part of the BT–BZ–CT system show both classical ferroelectric and relaxor ferroelectric behaviours. Their main characteristics vary as a function of composition. Two types of cationic substitutions (Ca^{2+}–Ba^{2+} and Zr^{4+}–Ti^{4+}) may account for this.

The value of T_C (or T_m) is almost constant as Ca^{2+} is substituted for Ba^{2+} (Table 1). Such a variation is due to several competition effects: a steric effect, a bonding effect and a coordination effect.[15] On the contrary, T_C (or T_m) decreases strongly as Zr^{4+} is substituted for Ti^{4+} (Table 1). This vari-

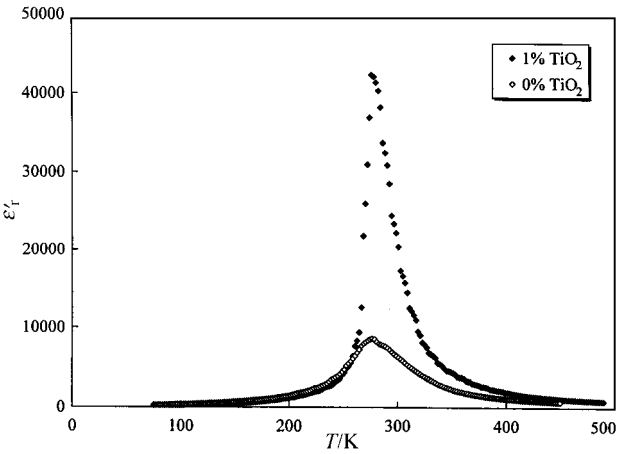

Fig. 10 Temperature dependences of relative permittivity ε'_r at 10^3 Hz for ceramics with composition corresponding to point F on Fig. 1, with or without 1 mol% TiO_2 additive.

Table 1 Variation of classical and relaxor ferroelectric characteristics with composition

Substitution	Composition	T_C[a]/K	T_m[a]/K	ΔT_m[b]/K	$\Delta\varepsilon'_r/\varepsilon'_r$[c]
Ca^{2+} for Ba^{2+}	$BaTiO_3$	400			0.06
	$Ba_{0.80}Ca_{0.20}TiO_3$	405			0.05
	$Ba(Ti_{0.85}Zr_{0.15})O_3$	340			0.07
	$Ba_{0.85}Ca_{0.15}(Ti_{0.85}Zr_{0.15})O_3$	347			0.03
	$Ba(Ti_{0.63}Zr_{0.37})O_3$		194	14	0.41
	$Ba_{0.88}Ca_{0.12}(Ti_{0.63}Zr_{0.37})O_3$		169	28	0.45
Zr^{4+} for Ti^{4+}	$BaTiO_3$	400			0.06
	$Ba(Ti_{0.80}Zr_{0.20})O_3$	314			0.05
	$Ba(Ti_{0.60}Zr_{0.40})O_3$		188	16	0.43
	$Ba_{0.90}Ca_{0.10}TiO_3$	410			0.05
	$Ba_{0.90}Ca_{0.10}(Ti_{0.90}Zr_{0.10})O_3$	364			0.06
	$Ba_{0.90}Ca_{0.10}(Ti_{0.70}Zr_{0.30})O_3$		209	19	0.37

[a]At 10^3 Hz. [b]$\Delta T_m = T_m(10^2\ \text{Hz}) - T_m\ (10^5\ \text{Hz})$. [c]$\Delta\varepsilon'_r/\varepsilon'_r = [\varepsilon'_r\ (10^2\ \text{Hz}) - \varepsilon'_r\ (10^5\ \text{Hz})]/\varepsilon'_r\ (10^2\ \text{Hz})$, at T_C (or T_m) − 50 K.

ation is related to the size of Zr^{4+} which is larger than that of Ti^{4+} ($r_{Ti^{4+}} = 0.605$; $r_{Zr^{4+}} = 0.72$ Å for six-coordination). This limits the shift (Δz) of the tetravalent cation from the octahedron center. Such an effect causes a decrease in T_C, owing to the variation of T_C with Δz: $T_C\,(\text{K}) = 2 \times 10^4\,(\Delta x)^2\,(\text{Å}^2)$.[16,17]

For small Zr^{4+} for Ti^{4+} substitution rates ($x \leqslant 0.15$, Fig. 1) no relaxor phase appears even for large amounts of Ca^{2+} (*e.g.* $Ba_{0.85}Ca_{0.15}Ti_{0.85}Zr_{0.15}O_3$ (Table 1)). This result is in good agreement with previous results: cationic substitution in the 12-coordinate crystallographic site has the classical ferroelectric behavior.[1,11] Concerning the substitution in the six-coordinate site, the equal charge of titanium and zirconium cations would require a high zirconium substitution rate ($x > 0.15$) to induce relaxor properties. Other substitutions, for instance Nb^{5+} for Ti^{4+} from $BaTiO_3$ in the $BaTiO_3$–$KNbO_3$ system, *i.e.* with a change of charge, leads to relaxor properties much more quickly.[12]

For a higher Zr^{4+} for Ti^{4+} substitution rate ($x > 0.15$) the relaxor phase appears. The main dielectric relaxor characteristics (ΔT_m and $\Delta\varepsilon'_r$, Table 1) increase as both the Zr–Ti and Ca–Ba substitution rates increase. This is due of course to the strong composition heterogeneity that exacerbates the relaxor effect. This was typically the case in the lead perovskite relaxor $Pb(Mg_{1/3}Nb_{2/3})O_3$ [PMN] where a local 1:1 order between niobium and magnesium atoms generated ordered regions surrounded by rich niobium polar regions. The heterogeneity thus created induced the relaxor effect commonly correlated with nanoscale spontaneous polarization.[1] The present result is of great interest for obtaining relaxor compositions at temperatures close to 300 K for use as lead-free capacitor dielectrics or actuators. As an example, the value of T_m corresponding to point E (Fig. 1) is 285 K (at 10^3 Hz), which can be compared to that of the well known but lead-containing PMN ($T_m = 266$ K).

The observed classical ferroelectric–relaxor transition at the wide composition boundary between zones II and III has been obtained in some relaxors, for instance in PMN, by application of an electric field inducing the ferroelectric phase by a cooperative mechanism creating a transformation from the nano- to the micro-domain structure.[18] In the present work the transition occurs spontaneously (without an applied electric field) just by temperature variation (Fig. 8). Until now, such a behaviour had been observed only in lead-containing relaxors: PSN, PST, PMN–PT solid solution, *etc.*[19,20]

Figs. 11 and 12 show the composition dependencies of transition temperatures for ceramics with either Ca^{2+} for Ba^{2+} or Zr^{4+} for Ti^{4+} substitutions. In the former the variation of T_m is weak, as discussed above when barium is replaced by calcium. In addition, a classical ferroelectric, $T_3 \rightarrow$relaxor ferroelectric transition occurs as soon as calcium enters the composition ($y > 0$) from that of the BT–BZ system ($BaTi_{0.74}Zr_{0.26}O_3$). In the second solid solution which starts from a composition of the BT–CT system, $(Ba_{0.90}Ca_{0.10})TiO_3$,

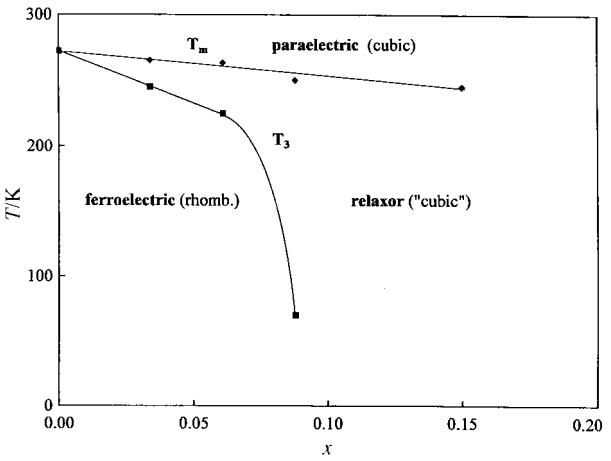

Fig. 11 Variation of transition temperatures with composition for $(Ba_{1-0.74x}Ca_{0.74x})(Ti_{0.74}Zr_{0.26})O_3$ solid solution ceramics.

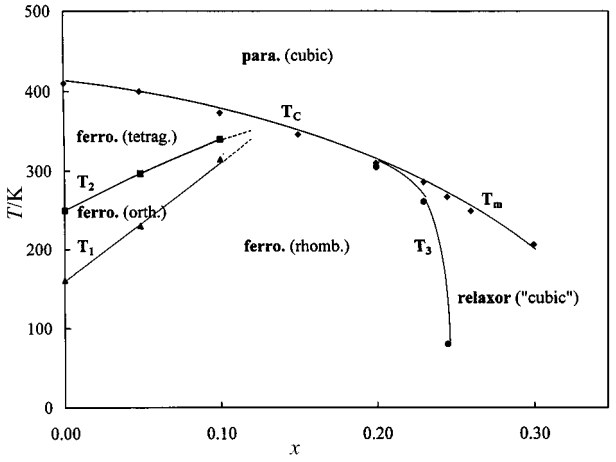

Fig. 12 Variation of transition temperatures with composition for $(Ba_{0.90}Ca_{0.10})(Ti_{1-0.90x}Zr_{0.90x})O_3$ solid solution ceramics

there is first a progressive disappearance of the tetragonal and orthorhombic ferroelectric phases, leading only to a rhombohedral, ferroelectric–cubic, paraelectric transition. Secondly, as observed earlier, a relaxor phase appears with a transition from relaxor to classical ferroelectric at T_3. Moreover in Fig. 12 it can be seen that the variation of T_C ($x \leqslant 0.2$) and then of T_m ($x \geqslant 0.2$) is stronger than in Fig. 11.

Conclusion

This relative permittivity study of ceramics with a composition inside the $BaTiO_3$–$BaZrO_3$–$CaTiO_3$ diagram shows a large

solid solution domain relatively close to $BaTiO_3$ with a derived perovskite structure. The ferroelectric behaviour is of a classical type for compositions close to that of $BaTiO_3$ or of relaxor type when they deviate from $BaTiO_3$. Owing to their relaxor behaviour at temperatures close to 300 K, some of these compositions could prove valuable (dielectrics for capacitors) because they are environmentally friendly.

A spontaneous classical ferroelectric–relaxor ferroelectric transition (without any applied electrical field) has now been evidenced in lead-free relaxors. Research is now underway to explain this potentially interesting behaviour.

References

1 L. E. Cross, *Ferroelectrics*, 1994, **151**, 305.
2 D. Hennings, A. Schnell and G. Simon, *J. Am. Ceram. Soc.*, 1982, **65**, 539.
3 V. V. Lemanov, N. V. Zaitseva, E. P. Smirnova and P. P. Syrnikov, *Ferroelectrics Lett.*, 1995, **19**, 7.
4 N. Yasuda, H. Ohwa and S. Asano, *Jpn. J. Appl. Phys.*, 1996, **35**, 5099.
5 Zhi Yu, Chen Ang, Zhi Jing, P. M. Vilarinho and J. L. Baptista, *J. Phys.: Condens. Matter*, 1997, **9**, 3081.
6 Y. M. Poplavko, *Key Eng. Mater.*, 1997, **132–136**, 1064.
7 Zhi Jing, Chen Ang, Zhi Yu, P. M. Vilarinho and J. L. Baptista, *J. Appl. Phys.*, 1998, **84**, 983.
8 J. Ravez and A. Simon, *Phys. Status Solidi*, 1997, **159**, 517.
9 J. Ravez and A. Simon, *C. R. Acad Sci.*, 1997, **325**, 481.
10 J. Ravez and A. Simon, *Eur. J. Solid State Inorg. Chem.*, 1997, **34**, 1199.
11 J. Ravez and A. Simon, *J. Korean Phys. Soc.*, 1998, **32**, 955.
12 J. Ravez and A. Simon, *Mater. Lett.*, 1998, **36**, 81.
13 T. Mitsui and W. B. Westphal, *Phys. Rev.*, 1961, **124**, 1354.
14 EIA RS-198, American Standard Requirements for Ceramic Dielectric Capacitors, classes 1 and 2, American Standards Association, New York, 1958.
15 J. Ravez, M. Pouchard and P. Hagenmuller, *Eur. J. Solid State Inorg. Chem.*, 1991, **28**, 1107.
16 R. D. Shannon, *Acta Crystallogr.*, *Sect. A*, 1968, **32**, 751.
17 S. C. Abrahams, S. K. Kurtz and P. B. Jamieson, *Phys. Rev.*, 1968, **172**, 551.
18 M. Chabin, M. Malki, E. Husson and A. Morell, *J. Phys. III*, 1994, **4**, 1151.
19 F. Chu, I. M. Reany and N. Setter, *Ferroelectrics*, 1994, **151**, 343.
20 F. Chu, I. M. Reany and N. Setter, *J. Appl. Phys.*, 1995, **77**, 1671.

Paper 9/02335F